Chemistry & Biology 13, 1081–1090, October 2006 ©2006 Elsevier Ltd All rights reserved DOI 10.1016/j.chembiol.2006.08.012

Design, Synthesis, and Biological Evaluation of Somatostatin-Based Radiopeptides

Mihaela Ginj,[1] Jörg S. Schmitt,[1] Jianhua Chen,[1] Beatrice Waser,[2] Jean-Claude Reubi,[2] Marion de Jong,[3] Stefan Schulz,[4] and Helmut R. Maecke[1,*]

[1] Division of Radiological Chemistry
Department of Radiology
University Hospital Basel
Petersgraben 4
4031 Basel
Switzerland

[2] Institute of Pathology
University Hospital Berne
3012 Berne
Switzerland

[3] Department of Nuclear Medicine
University Hospital Rotterdam
3015 GD Rotterdam
The Netherlands

[4] Department of Pharmacology and Toxicology
Otto-von-Guericke University
D-39106 Magdeburg
Germany

Summary

The prototypes for tumor targeting with radiolabeled peptides are derivatives of somatostatin. Usually, they primarily have high affinity for somatostatin receptor subtype 2 (sst2), and they have moderate affinity for sst5. We aimed at developing analogs that recognize different somatostatin receptor subtypes for internal radiotherapy in order to extend the present range of accessible tumors. We synthesized DOTA-octapeptides based on octreotide by replacing Phe3 mainly with unnatural amino acids. The affinity profile was determined by using cell lines transfected with sst1–5. Internalization was determined by using AR42J, HEK-sst3, and HEK-sst5 cell lines, and biodistribution was studied in rat tumor models. Two of the derivatives thus obtained showed an improved binding affinity profile, enhanced internalization into cells expressing sst2 and sst3, respectively, and better tumor:kidney ratios in animals.

Introduction

The tetradecapeptide somatostatin (SS-14) is of little therapeutic value despite its broad spectrum of biological actions, as it has a short half-life in vivo. Conformational analyses and structure-function studies on somatostatin analogs have indicated that the sequence required for biological activity consists of the β turn fragment Phe-Trp-Lys-Thr, which corresponds to residues 7–10 of SS-14 [1]. Many somatostatin analogs with smaller and more rigid rings have been synthesized in the search for compounds with enhanced and prolonged activity. Two lead compounds emerged from this research, the hexapeptide L-363,301 [1] and the octapeptide octreotide (Sandostatin, SMS 201-995) [2]. One unintended consequence of such structural simplification, which was carried out before the discovery of multiple receptor subtypes, was the loss of broad-spectrum binding affinity. The cloning of the five somatostatin receptors (sst1–sst5) [3] has increased the understanding of somatostatin receptor structure and function. It also revealed that the short-chain synthetic analogs of somatostatin have high affinity for somatostatin receptor subtype 2 (sst2), moderate to low affinity for sst3 and sst5, and no or very low affinity for sst1 and sst4.

In nuclear oncology, the prototypical tracers used for in vivo receptor scintigraphy and targeted radionuclide therapy are derivatives of somatostatin. The molecular basis for their use is the overexpression of somatostatin receptors on a variety of human tumors, especially neuroendocrine tumors and their metastases [4, 5]. The majority of human sst-positive tumors simultaneously express multiple sst subtypes, although there is a considerable variation in sst subtype expression between different tumor types and among tumors of the same type. Some of these differences are also due to the method used for investigating the occurrence of ssts [6]. Most of the hitherto available data on somatostatin receptor expression in human tumors originated from mRNA detection, but more recently several groups provided information on sst subtype protein expression [5, 7, 8]. Undoubtedly, subtype 2 is the most frequently expressed subtype in a majority of cancers. Nevertheless, in a significant number of tumors, sst2 is absent or expressed only in low density, whereas other ssts are present. For instance, frequent expression of sst1, sst2, sst3, and sst5 was found in gastro-entero-pancreatic tumors (GEP) [8], in medullary thyroid cancers (MTC) [9], and in ovarian cancers [10]. A predominant expression of sst3 was discovered in inactive pituitary adenomas, thymomas, and pheochromocytomas [5, 11, 12]. Human lung tumors were shown to overexpress sst2, sst3, and sst5 [13]. The considerable heterogeneity in the expression of individual ssts within and between different tumors provides evidence of the need for tracers that can target more than one sst in vivo.

The predominant expression of sst2 in human tumorous tissues forms the basis for the successful clinical application of radiolabeled octapeptide somatostatin analogs in the imaging of sst-positive tumors. The classical radioactive somatostatin analogs used for the in vivo visualization and treatment of human tumors are derivatives of octreotide, and the standard for scintigraphy is [^{111}In-DTPA]-octreotide (Octreoscan). Although remote from the pharmacophore, the addition of a metal complex to the N terminus of octreotide led to some loss in binding affinity, especially to sst5, but also to sst3 and sst2 [14]. Another derivative developed for nuclear medicine applications is [DOTA,Tyr3]-octreotide (DOTATOC), a conjugate that can be labeled with therapeutic radionuclides (e.g., ^{90}Y or ^{177}Lu); despite the selective

*Correspondence: hmaecke@uhbs.ch

Table 1. Affinity Profiles for Human Somatostatin Receptors 1–5, Hsst 1–5

Compound	Hsst1	Hsst2	Hsst3	Hsst4	Hsst5
SS-28	3.4 ± 0.3	2.7 ± 0.2	4.4 ± 0.4	3 ± 0.1	3.4 ± 0.3
M^{III}-1	>10,000	20 ± 2.2	27 ± 8	>1,000	58 ± 22
M^{III}-2	>10,000	11.4 ± 1.7	389 ± 136	>10,000	204 ± 92
M^{III}-3	>1,000	3.3 ± 0.2	26 ± 1.9	>1,000	10.4 ± 1.6
M^{III}-4	>10,000	25 ± 1.0	133 ± 68	>1,000	98 ± 12.5
M^{III}-5	>10,000	3.1 ± 0.3	12 ± 1.0	455 ± 65	6 ± 1.8
M^{III}-6	>10,000	22 ± 9	205 ± 43	>1,000	648 ± 165
M^{III}-7	>10,000	17 ± 6.6	617 ± 192	>1,000	647 ± 129
M^{III}-8	>10,000	47 ± 6.5	131 ± 69	>1,000	75 ± 45
M^{III}-9	>1,000	53 ± 16	649 ± 187	>1,000	>1,000
M^{III}-10	>10,000	85 ± 15	>1,000	>1,000	315 ± 105
M^{III}-11	>1,000	38 ± 2.0	52 ± 15	>1,000	283 ± 152
M^{III}-12	>10,000	39 ± 8.5	290 ± 160	>1,000	65 ± 7.0
M^{III}-13	>10,000	625 ± 25	>1,000	>1,000	495 ± 105
M^{III}-14	>10,000	4.0 ± 1.3	190 ± 10	>1,000	650 ± 250
M^{III}-15	>10,000	190 ± 50	>1,000	>1,000	775 ± 225
M^{III}-16	>10,000	12.3 ± 4.7	132 ± 18	960 ± 10	34 ± 3.0
M^{III}-17	>10,000	14 ± 1.5	22.7 ± 6.2	>1,000	137 ± 8.8
M^{III}-18	>1,000	161 ± 76	102 ± 53	187 ± 30	>1,000
M^{III}-19	>1,000	21 ± 1.0	47 ± 17	691 ± 99	20 ± 9.0
M^{III}-20	>1,000	93 ± 12	18 ± 1.0	>1,000	461 ± 163
M^{III}-21	>1,000	890 ± 74	119 ± 38	>1,000	>1,000
M^{III}-22	>10,000	>1,000	>10,000	>10,000	>1,000
M^{III}-23	>10,000	>1,000	>1,000	>1,000	>1,000
M^{III}-24	>10,000	285 ± 35	300 ± 130	>1,000	335 ± 5

IC_{50} values are expressed as mean ± SEM ($n \geq 3$); SS-28 is used as control. All compounds were complexed with either Y^{III} or In^{III}.

binding affinity only to sst2, this compound has been used clinically for about a decade [15]. Two other octreotide derivatives, lanreotide [16] and vapreotide [17], have been developed as well. These octapeptides have an improved binding affinity profile, but their metal-chelator conjugates display satisfactory affinity only to sst2 and sst5 [14].

Octreotide has been a subject of extensive structural studies, including NMR [18] and X-ray diffraction [19]. Taken together, these studies have demonstrated that octreotide exists in solution in two conformational families, differing mainly by the conformation of the C-terminal tail. The molecule adopts an overall antiparallel β sheet conformation, with a type II′ β turn centered at the D-Trp4-Lys5 region. In one conformational family, the residues after this β turn continue the β sheet structure, and in the second family, the residues after the β turn adopt a 3_{10} helical conformation. X-ray data of chelator-conjugated and metallated octapeptides are not yet available. ^{1}H- and ^{13}C-NMR data in solution are in agreement with the fast equilibrium of two predominant conformations, a helical and a β sheet structure, as in octreotide [20]. All of the peptidic analogs of octreotide conserve the critical sequence D-Trp4-Lys5, and only subtle modifications have been done to the side chain amino acids of this β turn (Phe3 and Thr6) [21]. Among the clinically used analogs of somatostatin (octreotide, lanreotide, and vapreotide) the only modification carried out in the third position has been the substitution of Phe3 (in octreotide) with Tyr3 (in lanreotide and vapreotide). Since this substitution is accompanied by other structural changes at the C terminus (Thr-NH_2 in lanreotide, Trp-NH_2 in vapreotide versus Thr(ol) in octreotide) and/or the N terminus (D-2-Nal in lanreotide instead of D-Phe in octreotide and vapreotide), as well as at the sixth residue (Thr in octreotide replaced by Val in lanreotide and vapreotide), it is difficult to assess the alterations in the binding affinity profile. Still, a direct comparison of the effects produced by the replacement of Phe3 with Tyr3 is noticeable on the metal-chelator conjugates Y^{III}-DOTA-octreotide (Y^{III}-DOTA-OC) and Y^{III}-DOTA-[Tyr3]-octreotide (Y^{III}-DOTA-TOC) [14] (also see Table 1). The more hydrophilic conjugate with Tyr on the third position has increased binding affinity for sst2, but it has decreased binding potency to sst3 and sst5.

Based on these structural and empirical data, we assumed that modifications at this position in metal-complexed DOTA derivatives of octreotide might modulate the affinity profile to sst3 and sst5. Our premise was that bulky aromatic residues would improve the binding affinity for sst3 and sst5 without compromising the binding potency to sst2. The generation of radioactive conjugates with a broader affinity profile would not only lead to an extension of the present range of targeted cancers, but it would also mean an increased dose of radioactivity to the tumor, given the presence of different receptor subtypes on the same tumor cell or in the same tumor entity.

In this paper, we describe the synthesis and pharmacological evaluation of a small library of metal-DOTA-peptides derived from octreotide with modifications at the third amino acid residue. We have already reported the first compound resulting from this library, [^{111}In/^{90}Y-DOTA]-NOC, which has improved biological properties and is currently in clinical trials [22].

Results and Discussion

The DOTA-somatostatin analogs **1–24** (Figure 1) obtained by systematic modification of aa^3 in octreotide were synthesized by parallel synthesis on solid phase

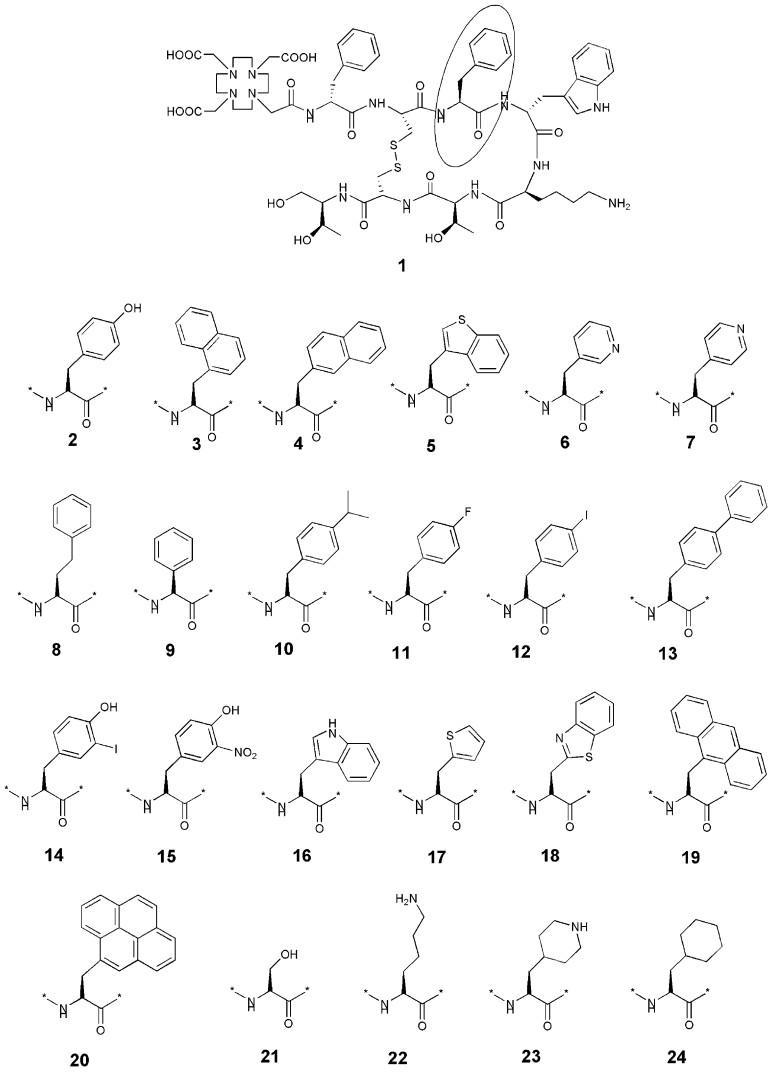

Figure 1. Structural Formulae of Conjugates **1–24**

by using the Fmoc/*t*Bu strategy and the 2-chloro-trityl-chloride linker. After cleavage from the resin, cyclization in solution, and total deprotection, the crude products were obtained in 25%–30% yield based on the first Fmoc cleavage. All peptide conjugates had a purity of >97%, confirmed by RP-HPLC analysis. In each case, the ESI-MS spectra consisted of a major $[M+2K]^{2+}$ ion peak and two minor peaks corresponding to $[M+K]^{+}$ and $[M+3K]^{3+}$ ions (Table S1, see the Supplemental Data available with this article online). Metal-ion-complexed DOTA-peptides were characterized by HPLC, MS-ESI, and by the retained affinity for the somatostatin receptors. Labeling with ^{111}In was performed in acetate buffer (pH 5, 0.4 M) by heating at 95°C for 25 min, affording >99% labeling yields at a specific activity of >37 GBq/μmol peptide.

The partition coefficients of the $^{111/115}$In-labeled derivatives **1–24** between aqueous (PBS, pH 7.4) and organic (octanol) layers were determined by using the shake flask method. The results are displayed in Figure 2; the most lipophilic compound is $^{111/115}$In-**20**, and the most hydrophilic ones are $^{111/115}$In-**22** and -**23**.

Table 1 shows the IC_{50} values of the conjugates studied in this work as their Y^{III}- or In^{III}-complexed versions for the five ssts. The values were obtained by performing complete displacement experiments with the universal somatostatin radioligand [^{125}I][Leu8, D-Trp22, Tyr25]-somatostatin-28 on membranes from cells expressing the receptor subtypes and were compared to those of SS-28.

Internalization studies were performed on AR42J rat pancreatic tumor cells and on HEK cells stably expressing sst3 and sst5 receptors, respectively. The uptakes in the first two cell lines after a 4 hr incubation with the radiopeptides are shown in Table 2. These values represent specific accumulation, i.e., the difference between total uptake and nonspecific accumulation in the presence of excess nonradioactive derivatives.

We arranged compounds **1–24** in various classes according to the nature of the amino acid in the third position of the peptide sequence. The following discussion concentrates on these categories.

Phe Derivatives

Comprising the parent compound, DOTA-octreotide, are six conjugates bearing a phenylalanine derivative in the third position of the peptide: **1**, **8**, **9**, **10**, **11**, and **12**. In the homolog series **9**, **1**, and **8**, no improvement

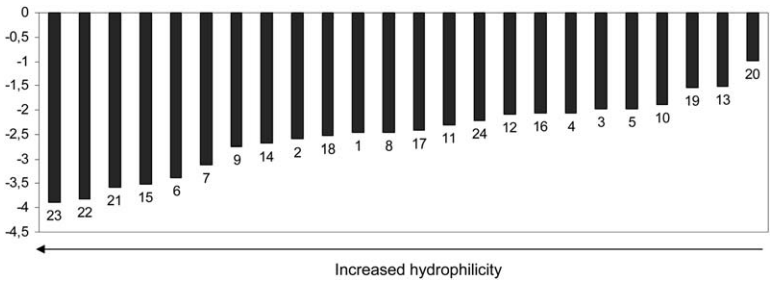

Figure 2. Schematic Illustration of the Partition Coefficient Values for the $^{111/115}$In-Labeled Conjugates **1–24**

either in binding affinity or in internalization occurs by varying the length of the side chain. Although the phenylglycine residue was previously successfully employed in this position of the β turn in the cyclohexapeptide analog of somatostatin SOM-230 [23], its incorporation in DOTA-octapeptide **9** caused a complete loss of affinity for sst3 and sst5, and a 2.5-fold drop for sst2. The superior Phe homolog derivative **8** retained some affinity for sst2, sst3, and sst5, but this affinity was lower than that of **1**. Also, the internalized amount in cells expressing the rat sst2 receptor (AR42J) is lower compared to **1**. The two halogeno-Phe derivatives **11** and **12**, while displaying comparable lipophilicities, the same binding affinities to sst2, and similar amounts of internalized radiopeptide in AR42J cells at 4 hr, differ significantly in their binding potencies for sst3 and sst5, respectively. In-**11** had higher binding affinity for sst3 than In-DOTA-octreotide, and it also had a superior accumulation in HEK-sst3 cells. Derivative **10**, the most lipophilic of this series, had the highest accumulation in AR42J cells but the lowest sst2 binding affinity among the six conjugates of this group.

Table 2. Internalization of ^{111}In-Labeled Peptides **1–24** in AR42J Cells Expressing Sst2 and in HEK Cells Expressing Sst3 after a 4 hr Incubation at 37°C

Radiopeptide	Percentage Internalized in AR42J Cells	Percentage Internalized in HEK-Rsst3 Cells
^{111}In-**1**	6.1 ± 0.5	1.8 ± 0.7
^{111}In-**2**	11.5 ± 1.8	0.8 ± 0.2
^{111}In-**3**	25.0 ± 1.5	16.3 ± 1.9
^{111}In-**4**	0.9 ± 0.3	0.5 ± 0.2
^{111}In-**5**	17.2 ± 1.9	24.3 ± 0.9
^{111}In-**6**	1.1 ± 0.8	<0.1
^{111}In-**7**	1.5 ± 0.3	<0.1
^{111}In-**8**	1.9 ± 0.6	2.0 ± 0.1
^{111}In-**9**	0.7 ± 0.4	0.3 ± 0.1
^{111}In-**10**	12.7 ± 1.2	<0.1
^{111}In-**11**	3.7 ± 0.3	5.3 ± 0.1
^{111}In-**12**	5.3 ± 0.7	1.2 ± 0.1
^{111}In-**13**	<0.1	<0.1
^{111}In-**14**	5.0 ± 0.4	1.2 ± 0.2
^{111}In-**15**	0.8 ± 0.2	<0.1
^{111}In-**16**	5.3 ± 0.3	<0.1
^{111}In-**17**	7.2 ± 0.6	12.6 ± 1.2
^{111}In-**18**	0.5 ± 0.3	<0.1
^{111}In-**19**	2.7 ± 0.4	6.8 ± 0.3
^{111}In-**20**	2.4 ± 0.5	12.1 ± 1.0
^{111}In-**21**	<0.1	0.8 ± 0.5
^{111}In-**22**	<0.1	<0.1
^{111}In-**23**	<0.1	<0.1
^{111}In-**24**	0.6 ± 0.3	<0.1

The results are expressed as % specific internalized from the total added radioactivity per one million cells (mean ± SD; n = 3).

Tyr Derivatives

The presence of a weak (-I, conjugate **14**) and a strong (-NO_2, conjugate **15**) electronic deactivator, respectively, on the Tyr ring in the ortho position relative to the phenolic OH causes an increase in the pKa values of these residues (data not shown). This is reflected in the partition coefficients, which increase in the order **2** ≥ **14** >> **15**. Apparently, a more acidic residue in this position is not beneficial either to the binding affinities to any of the ssts or to the internalization into sst2- or sst3-expressing cells; $^{111/115}$In-**15** shows a net inferior biological profile when compared with $^{111/115}$In-DOTA-TOC ($^{111/115}$In-**2**). Using the same reference, $^{111/115}$In-**14** has a lower internalization rate in AR42J cells but an improved sst2 affinity. This result does not corroborate the previous findings of Hofland et al. [24] on [DOTA,^{125}I-Tyr3]-octreotide, which showed an increased uptake in sst-expressing cells and tissues.

Heterocyclic Side Chain Derivatives

Seven residues with a heterocyclic side chain have been introduced in the third position of octreotide: two pyridine derivatives (**6** and **7**), a thiophene (**17**), a benzothiophene (**5**), an indole (**16**), a benzthiazole (**18**), and a piperidine side chain residue (**23**). Undoubtedly, the best biological profile in this series belongs to M^{III}-**5**, the most lipophilic of this group. Moreover, it also shows a significant increase in binding affinity for sst2. The internalizations in sst2- and sst3-expressing cells mirror these results. Its N analog (**16**) shows comparable lipophilicity, but significantly lower potency on sst2 and sst5, as well as a dramatic drop of binding affinity and internalization rate toward sst3. Interestingly, the somewhat more hydrophilic related conjugate **18** fails in all biological assays. The thiophenylalanine derivative **17** has a reasonable sst2 and sst3 binding profile and a moderate rate of internalization in both cell lines studied. The two pyridinylalanine derivatives, **6** and **7**, preserve a satisfactory affinity for sst2, but they induce poor endocytosis in AR42J cells. In the structure-activity investigations done by Hocart et al. [25] in their search for somatostatin antagonists, the substitution of 3-pyridylalanine in this position produced an antagonist with marginal affinity for sst2 (291 nM). The worst derivative of this series is the most hydrophilic one, bearing a piperidylalanine residue in the third position (**23**).

Polyaromatic Side Chain Derivatives

Two naphthylalanine derivatives (**3** and **4**), a diphenylalanine (**13**), an anthranylalanine (**19**), and a pyrenylalanine (**20**) have been employed instead of Phe3 in octreotide. The complexed version of **3** has incontestably the best

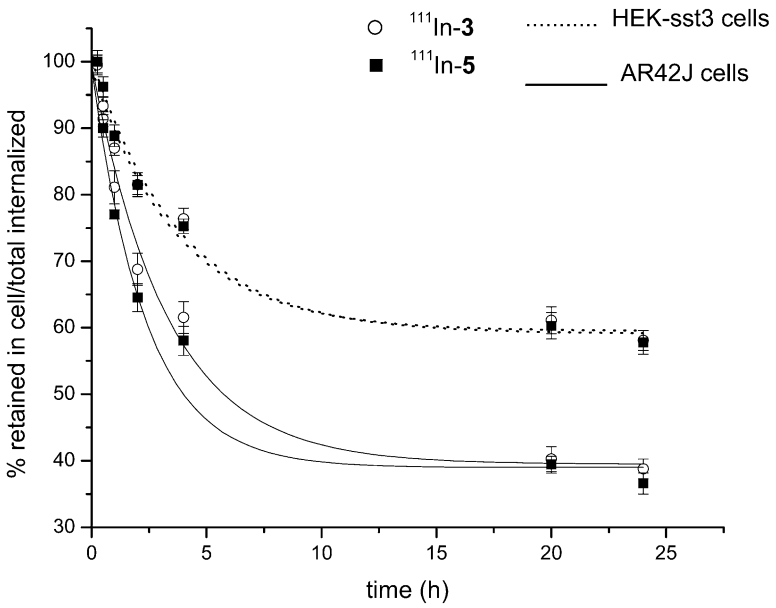

Figure 3. Comparison in Cellular Retention after 2 hr of Internalization of ^{111}In-3 and ^{111}In-5 in AR42J Cells and in HEK Cells Expressing sst3

The values represent the percentage retained in the cell of the total amount internalized (mean ± SD, n = 3).

biological profile of this group [22]. The binding potency of this compound on sst2 and sst3 is complemented by good internalization rates in cells expressing these receptors. It has also a superior binding affinity for sst5 compared with the parent conjugate **1**. Interestingly, the 2-Nal[3] conjugate (**4**) turned out to be inferior in all assays, a result difficult to explain, given the very small structural difference between the two compounds. It has moderate binding affinity for sst2, comparable with that of **1**, and shows insignificant accumulation in AR42J cells after a 4 hr incubation at 37°C. The diphenyl-substituted derivative **13**, one of the most lipophilic conjugates of this series, completely loses binding affinity for all ssts and thus the capacity to activate the internalization of the receptors as well.

The bulkiest and most lipophilic conjugate, **20**, has one of the highest affinities to sst3, and it also induces one of the highest internalization rates in HEK-sst3 cells. The second bulkiest conjugate, **19**, has lower affinity for sst3, but higher affinity for sst5, while it also maintains a good binding affinity for sst2.

Aliphatic Side Chain Derivatives

The three aliphatic side chain residues Ser (**21**), Lys (**22**), and cyclohexylalanine (**24**) were employed in the third position for reasons of comparison and to prove the necessity of an aromatic residue in this location. All of these derivatives lost their binding affinity for all sst subtypes and did not internalize in either sst2- or sst3-expressing cells. Previous Ala-scan studies [26] on SS-14 have also shown that the replacement of Phe7 (corresponding to Phe3 in octreotide) by an Ala residue leads to a drop of ~90% in the ability to inhibit growth hormone release in vitro. For derivative **22**, as for the above-mentioned conjugate **23**, another reason for the loss of potency might be due to the additional positive charge.

Summarizing the above-presented data, very subtle modifications in the region of the β bend have profound effects on the pharmacological profile. Even if the binding affinity and the capacity to internalize are two distinct features of a G protein-coupled receptor that do not necessarily correlate [27], most of the ligands with reasonable-to-good binding affinity reported herein also induce internalization to a higher or lower extent. Two intriguing exceptions to this "rule" are the metal-complexed derivatives **4** and **10**, as depicted above. Given the complex signal transduction mechanisms of somatostatin receptors [27], it is difficult to explain these results; however, they are probably due to the different agonist abilities (partial or total agonist) of these derivatives. Substantial evidence points to ligand composition, receptor subtype, and the cell line used for transfection of receptor DNA as critical factors in the intracellular routing and retention of somatostatin and its analogs [28].

Generally, the bulky and lipophilic residues employed instead of Phe3 increase the binding affinity for sst3 and also activate the internalization of this receptor. The best conjugates for this receptor were the metal-complexed **3**, **5**, **17**, **19**, and **20** conjugates. Some of them also enhance the potency of binding to sst5 (**3**, **5**, **16**, and **19**).

Nevertheless, the broadest affinity profile in this series, supplemented by a good activation of internalization in sst2- and sst3-expressing cell lines, respectively, was shown by the metal-complexed conjugates **3** and **5**. We previously reported the biological evaluation of $^{111/115}$In-**3** ($^{111/115}$In-DOTA-NOC) [22] compared to $^{111/115}$In-labeled DOTA-TOC and DOTA-OC. This compound is currently being clinically studied in a group of metastasized thyroid cancer patients not showing radioiodine uptake anymore; compared to the other radiolabeled somatostatin analogs in clinical use, it shows improved imaging properties [29].

We compared ^{111}In-**5** with ^{111}In-**3** in cellular retention tests in AR42J and HEK-sst3 cells (Figure 3), and we found a similar behavior in both cell lines. Both compounds display a higher retention of the internalized fraction in the sst3-expressing cells than in sst2-expressing cells, which is probably due to the difference in receptor dynamics: after agonist-induced internalization, sst2 receptors have been shown to recycle rapidly

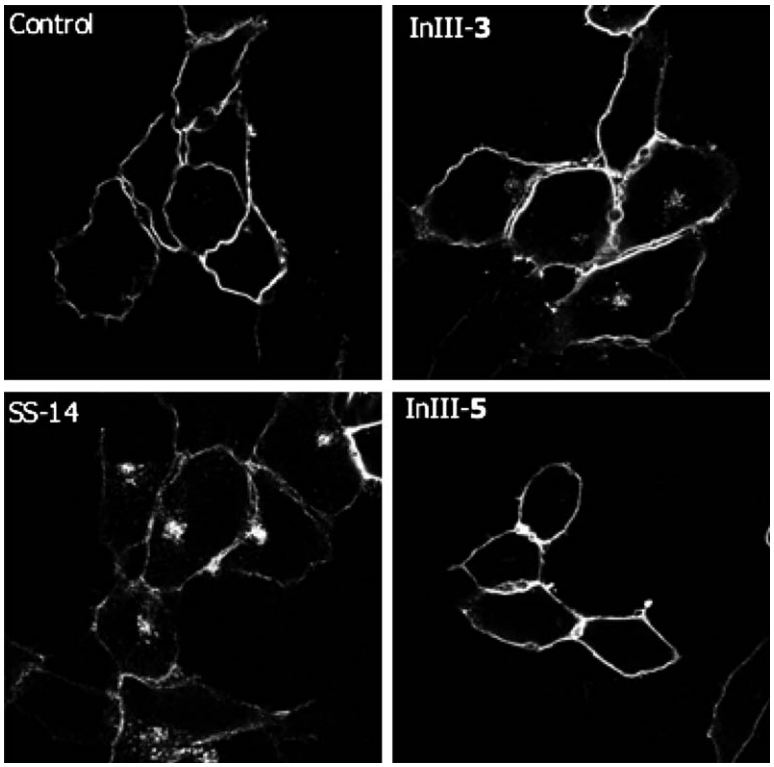

Figure 4. Agonist-Induced Receptor Internalization in HEK Cells Expressing sst5

Agonist-induced receptor internalization: HEK cells stably expressing human sst5 were exposed for 30 min to SS-14, In^{III}-**3**, and In^{III}-**5**. Cells were then fixed, processed for immunofluorescence, and examined by confocal microscopy. Shown are representative images from one of three independent experiments performed in duplicate. The scale bar is 20 μm.

to the plasma membrane, whereas sst3 receptors suffer lysosomal degradation and hence do not recycle rapidly to the plasma membrane [30]. Nevertheless, the two conjugates behave differently in immunocytochemical internalization studies in HEK cells stably expressing human sst5 receptors (Figure 4). Although it has previously been shown by Roth et al. [28] that in sst5-transfected HEK cells receptor endocytosis is promoted only by the octacosapeptide (SS-28), and not by SS-14, in our assay SS-14 triggers receptor internalization after 30 min of incubation at 37°C. Also, In^{III}-**3** induces sst5 internalization in HEK-sst5 cells to a lower extent than SS-14, while In^{III}-**5** activates no receptor endocytosis in these cells. In our radioligand assays of internalization in HEK-sst5 cells, no uptake has been found for any of the radiopeptides, including ^{111}In-**3** and -**5** (data not shown).

In vitro internalization studies are generally used as a predictor of in vivo tumor or sst-positive tissue accumulation [31]. Despite the negative results obtained in the sst5 internalization assays, ^{111}In-**5** has a 2-fold higher accumulation than ^{111}In-**3** in CA20948 rat pancreatic tumor (Figure 5A) at 4 hr after injection. This ratio between the two ligands is also maintained 24 hr after injection, and it slightly decreases after 48 hr. As this type of tumor has been shown to express several ssts [32], sst homo- and heterodimerization may alter both ligand affinity and signaling efficacy of somatostatin receptors in these tumor cells [33, 34]. In the AR42J tumor, the two ligands accumulate in a similar manner (Figure 5B) as a consequence of the sole sst2 presence in this tissue [35]. Both radioligands have favorable tumor:kidney ratios in both rat tumor-bearing models, as shown in Figure 5 [22]. This is an important parameter in targeted radiotherapy since the kidney is the dose-limiting organ [36].

Overall, in addition to DOTA-NOC (**3**), conjugate **5** (named DOTA-BOC), originating from the same library of DOTA-octreotide derivatives with modifications at the third residue, displays very promising preclinical

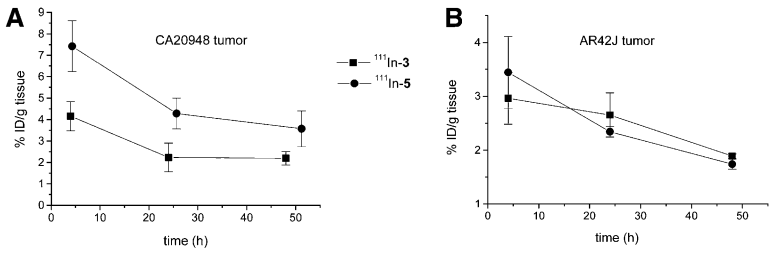

	CA20948 model	
Tumor:kidney	^{111}In-**3**	^{111}In-**5**
4h	2.0 ± 0.6	2.23 ± 0.3
24h	1.2 ± 0.3	1.44 ± 0.24
48h	1.12 ± 0.2	1.27 ± 0.29

	AR42J model	
Tumor:kidney	^{111}In-**3**	^{111}In-**5**
4h	2.1 ± 0.35	1.77 ± 0.3
24h	2.08 ± 0.3	1.42 ± 0.05
48h	1.5 ± 0.03	1.1 ± 0.06

Figure 5. Comparison between ^{111}In-**3** and ^{111}In-**5** in Tumor Uptake and Tumor:Kidney Ratios

(A and B) Comparison of the tumor uptake kinetics and the tumor:kidney ratios (mean ± SD) between ^{111}In-**3** and ^{111}In-**5** in two animal models: (A) CA20948 and (B) AR42J (*$p < 0.001$, compared with the uptake of the other compound; $n \geq 3$).

data. We have recently reported the synthesis and biological evaluation of the Thr8 modification of these conjugates (DOTA-NOC-ATE and DOTA-BOC-ATE), which also show encouraging in vitro and in vivo biological profiles but a somewhat faster tumor washout compared with ^{111}In-3 and ^{111}In-5 [37]. As mentioned, this type of radioligand might be used as an imaging agent to predict the usefulness of a therapy with cold octreotide (Sandostatin) or lanreotide (Somatuline) rather than with OctreoScan, which has a much less adequate binding profile for this purpose. Since there is no radioligand for SOM230—a cyclohexapeptide that has high binding affinity for sst1, sst2, sst3, and sst5 and is currently under evaluation in phase 1 clinical trials [38]—these radioligands may also be candidates for identifying patients eligible for SOM230 treatment.

Significance

Peptide receptor-mediated radionuclide imaging and targeted therapy are emerging fields in oncology. The prototypical peptides are derivatives of somatostatin. Nevertheless, the clinically used derivatives primarily have affinity for sst2. Although this receptor is overexpressed in a variety of tumors, there are several malignancies with other ssts being expressed in higher density. We designed and synthesized a new, to our knowledge, series of DOTA-octreotide derivatives by exchanging the third residue in octreotide principally with a variety of aromatic side chain amino acids. We chose this position due to its involvement in the critical β turn of this molecule and to the empirical observations on the pharmacological profile of two DOTA derivatives used in the clinic. The small library of compounds thus obtained is not only a useful structure-activity investigational tool, but it also provides two new, to our knowledge, derivatives with improved pharmacological properties. DOTA-[1-Nal^3]-octreotide (3) and DOTA-[BzThi^3]-octreotide (5), when labeled with ^{111}In, ^{90}Y, ^{177}Lu, or ^{68}Ga, have the broadest affinity profile among the radioligands used in the clinic and can efficiently target sst2, sst3, and sst5. This means not only an increase of the present range of targeted tumors, but also an enhanced cytotoxic radioactive dose to the same tumor expressing several ssts.

Experimental Procedures

Abbreviations

The nomenclature for the somatostatin receptor subtypes (ssts) is in accordance with the recommendations of IUPHAR [3]. Abbreviations of the common amino acids are in accordance with the recommendations of IUPAC-IUB [39]. Additional abbreviations: 1 (or 2)-Nal, 1 (or 2)-naphthylalanine; Thi, (2-thienyl)-alanine; 3 (or 4)-Pya, 3 (or 4)-pyridylalanine; hPhe, homophenylalanine; (4-I) Phe, 4-iodophenylalanine; (4-iPr) Phe, 4-isopropyl-phenylalanine; (3-NO_2) Tyr, 3-nitro-tyrosine; (4-Pip) Ala, 4-piperidinyl-alanine; BzThi, 3-benzothienylalanine; Cha, cyclohexylalanine; Antra, anthranylalanine; Pyra, 1-pyrenylalanine; PhGly, phenylglycine; DOTA, 1,4,7,10-tetraazacyclododecane-1,4,7,10-tetraacetic acid; DOTA($tBu)_3$ (prochelator), 1,4,7,10-tetraazacyclododecane-1,4,7-tris(*tert*butyl acetate)-10-acetic acid; DCM, dichloromethane; DIC, diisopropylcarbodiimide; DIPEA, diisopropylethylamine; DMF, dimethylformamide; HOBt, *N*-hydroxybenzotriazole; HATU, O-(7-azabenzotriazol-1-yl)-*N*, *N*, *N*′, *N*′-tetramethyluroniumhexafluorophosphat; TFA, trifluoroacetic acid; TFE, trifluoroethanol; TIS, triisopropylsilane; TNBS, 2,4,6-trinitrobenzenesulphonic acid.

Materials

All chemicals were obtained from commercial sources and were used without further purification. H-Thr(tBu)ol-(2-chlorotritylchloride) resin was obtained from Advanced ChemTech (Louisville, KY), and most Fmoc (9-fluorenylmethoxycarbonyl) amino acids were purchased from NovaBiochem AG, Läufelfingen (Switzerland) and Neosystem (France). The reactive side chains of the amino acids were masked with one of the following groups: Cys, acetamidomethyl; Lys, *t*-butoxycarbonyl; Thr, *t*-butyl; Trp, *t*-butoxycarbonyl. The prochelator DOTA($tBu)_3$ was synthesized according to Heppeler et al. [40]. Analytical RP-HPLC was carried out on a Hewlett Packard 1050 HPLC-system equipped with a multiwavelength-detector and a flow-through Berthold LB506C1 γ-detector. Preparative HPLC was done on a Bischof HPLC system (Metrohm AG, Switzerland) with HPLC-pumps 2250 and a Lambda 1010 UV-detector. Quantitative γ-counting was performed on a COBRA 5003 γ-system well counter from Packard Instrument Company (Switzerland). Electrospray ionization-mass spectrometry (ESI-MS) was carried out with a Finnigan SSQ 7000 spectrometer (Bremen, Germany). $^{111}InCl_3$ was obtained from Mallinckrodt Medical (Petten, The Netherlands).

Peptide-Conjugate Synthesis

The peptide-chelator conjugates were synthesized by parallel standard Fmoc-solid-phase synthesis [41] on 2-chlorotritylchloride resin (substitution 0.8 mmol/g) on a Rink Engineering peptide-synthesizer Switch 24 (RinkCombichem, Bubendorf, Switzerland). A 3.0 equivalent excess of the protected amino acids based on the original substitution of the resin was used. The couplings were mediated by DIC and HOBt in DMF for 1 hr and were monitored by the qualitative ninhydrin or TNBS test. Fmoc removal was achieved with 20% piperidine in DMF in two successive 10 min treatments. The last step on the solid phase was the coupling of the prochelator DOTA($tBu)_3$ to the N terminus of the peptide for 2 hr, by using HATU as an activating agent. The fully protected conjugates were then cleaved from the resin support by using a 1% TFA in DCM solution also containing H_2O (0.5% v/v) and TFE (20% v/v) as scavengers (30 ml cleavage cocktail/mmol equivalent resin). After coevaporation with toluene and drying in a desiccator, the crude protected peptide conjugates were cyclized in aqueous MeOH by the addition of iodine (10 equivalents of a 0.25 M I_2 solution). Thirty minutes later, a 0.5 M solution of ascorbic acid was added to quench the excess of iodine. For complete deprotection, the dried, cyclized peptide conjugates were dissolved in TFA with TIS (3% v/v), thioanisole (3% v/v), and H_2O (5% v/v) as scavengers (15 ml/mmol). After a 4 hr incubation at room temperature, the crude products were precipitated with cold diethyl ether.

Purification and Characterization of Peptide Conjugates

The crude conjugates were purified by preparative RP-HPLC by using an Interchrom Uptisphere 5ODB C18 column (250 × 21.2 mm) and a linear gradient from 20% to 50% solvent B (solvent A, 0.1% TFA/water; solvent B, acetonitrile) over 25 min at a flow rate of 15 ml/min. Detection was done at 254 nm. All compounds were lyophilized after purification and characterized by ESI-MS and HPLC. Pure compounds were identified by analytical multiwavelength RP-HPLC with a CC250/4 Nucleosil 120-3C18 column from Macherey-Nagel by using a linear gradient from 10% B to 60% B over 40 min at a flow rate of 0.75 ml/min (solvent A, 0.1% TFA/water; solvent B, acetonitrile).

Formation of Metal Complexes

The DOTA-SRIF-analogs were complexed either with $InCl_3$ (anhydrous) or $Y(NO_3)_3 \cdot 5\ H_2O$, as described by Wild et al. [22]. The radiolabeling of these peptide conjugates was also done according to Wild et al. [22], and the radiopeptides were obtained in >99% radiochemical purity at specific activities of >37 GBq/μmol peptide. For internalization, cellular retention, and animal biodistribution experiments the DOTA-peptides were labeled with $^{111}InCl_3$ to a specific activity of about 37 GBq/μmol peptide, and then excess $^{115}InCl_3$ was added to afford structurally characterized homogenous ligands.

Determination of Lipophilicity

The octanol-water partition coefficients were determined by using the shake flask method. Both solvents (aqueous and octanol) were presaturated with the other by leaving them in contact for at least 24 hr. To a solution of 100 nM radiolabeled peptide (6 MBq/nmol) in 500 μl PBS (pH 7.4), 500 μl octanol were added (n = 5). The mixtures were vigorously shaken on a shaker long enough to reach equilibrium (~1 hr). After equilibration, the mixtures were centrifuged (10 min at 2000 rpm) to achieve good separation. The activity concentrations in 100 μl samples of both the aqueous and the organic phase were measured in a γ-counter. The partition coefficient (log P) was calculated from the formula:

$$\log P = \log_{10}(\text{counts in octanol layer}/\text{counts in aqueous layer}).$$

Receptor Binding Assays

CHO-K1 and CCL39 cells stably expressing human sst1–5 were grown as described previously [14]. All culture reagents were supplied by GIBCO-BRL and Life Technologies (Grand Island, NY). Cell membrane pellets were prepared, and receptor autoradiography was performed on pellet sections (mounted on microscope slides), as described in detail previously [14]. For each of the tested compounds, complete displacement experiments were performed with the universal somatostatin radioligand [^{125}I][Leu8, D-Trp22, Tyr25]-somatostatin-28 by using increasing concentrations of the Metallo^{III}-DOTA-peptide ranging from 0.1 to 1000 nM. Somatostatin-28 was run in parallel as a control by using the same increasing concentrations. IC_{50} values were calculated after quantification of the data by using a computer-assisted image processing system. Tissue standards (autoradiographic [^{125}I] microscales; Amersham, UK) containing known amounts of isotopes, crosscalibrated to tissue-equivalent ligand concentrations, were used for quantification [14].

Cell Culture, Radioligand Internalization, and Cellular Retention Studies

The apparatus and procedures for cell internalization and cellular retention experiments are based on previously described methods [37]. Briefly, the AR42J cell line was maintained by serial passage in monolayers in Dulbecco's modified Eagle's media (DMEM), supplemented with 10% fetal bovine serum, amino acids, vitamins, and penicillin-streptomycin, in a humidified 5% CO_2 atmosphere at 37°C. Human embryonic kidney 293 (HEK293) cells stably expressing rat sst3 receptors [30] were grown in DMEM supplemented with 10% fetal bovine serum, penicillin-streptomycin, and G418 (500 μg/ml) in a humidified 5% CO_2 atmosphere at 37°C. For all cell experiments, the cells were seeded at a density of 0.8–1.1 million cells/well in 6-well plates and were incubated overnight with internalization buffer (DMEM, 1% fetal bovine serum [pH 7.4]) to obtain a good cell adherence. The $^{111/115}$In-labeled peptides were added to the wells to a final concentration of 1.67 nM, and the cells were incubated at 37°C for the indicated time periods in triplicate. To determine nonspecific membrane binding and internalization, cells were incubated with the radioligand in the presence of 1 μM In^{III}-**3**. The cellular uptake was stopped by removing the medium from the cells and by washing the cells twice with 1 ml ice-cold PBS. An acid wash for 10 min with a glycine-buffer (pH 2.8) on ice was also performed twice. Finally, the cells were treated with 1 N NaOH. The culture medium, the surface-bound fraction, and the internalized fraction were measured radiometrically in a γ-counter.

For cellular retention studies AR4-2J cells as well as HEK cells stably expressing sst3 (1 million) were incubated with 1.67 nM $^{111/115}$In-labeled **3** and **5** for 120 min, respectively, the medium was then removed, and the wells were washed twice with 1 ml ice-cold PBS. Cells were then incubated again at 37°C with fresh internalization buffer (DMEM containing 1% fetal bovine serum [pH 7.4]). After different time points, the external medium was removed for quantification of radioactivity in a γ-counter and was replaced with fresh 37°C medium. The cells were solubilized in 1 N NaOH, and the internalized radioactivity was quantified in a γ-counter. The washed-out fraction collected at different time points was expressed as a percentage of the total internalized amount of radiopeptide per 1 million cells.

Immunocytochemistry

HEK293 cells were stably transfected with the human sst5 receptor, as previously described [30]. After 30 min of treatment with 1 μM SS-14, In^{III}-**3**, or and In^{III}-**5**, cells were fixed with 4% paraformaldehyde and 0.2% picric acid in phosphate buffer (pH 6.9) for 40 min at room temperature and were washed three times in 10 mM Tris-HCl (pH 7.4), 10 mM phosphate buffer, 137 mM NaCl, and 0.05% thimerosal (TPBS). Specimens were then incubated for 3 min in 50% methanol and for 3 min in 100% methanol, washed in TPBS, and preincubated with TPBS supplemented with 3% normal goat serum for 1 hr at room temperature. Cells were then incubated with affinity-purified anti-sst5 antibody obtained as previously described [42] at a concentration of 1 μg/ml in TPBS supplemented with 1% normal goat serum overnight. After washing with TPBS, bound primary antibody was detected with cyanine 3.18-conjugated secondary antibody (Amersham, Braunschweig, Germany). Specimens were mounted and examined with a Leica TCS-NT laser scanning confocal microscope as described [42].

Animal Biodistribution Studies

Animals were kept, treated, and cared for in compliance with the guidelines of the Swiss regulations (approval #789).

CA20948 Rat Tumor Model

Male Lewis rats (Harlan, The Netherlands; 200–300 g), bearing the rat CA20948 pancreatic tumor [31] in their flank, were used for the experiments. An injection of 2–3 MBq of 0.34 nmol (0.5 μg total peptide mass) ^{111}In-**3** or ^{111}In-**5** in 0.1 ml saline was administered to the dorsal vein of the penis of ether-anesthesized rats.

AR42J Rat Tumor Model

Five-week-old male Lewis rats were implanted subcutaneously with 10–12 million AR4-2J cells freshly suspended in sterile PBS. Fourteen days after inoculation, the rats showed solid palpable tumor masses (tumor weight of 0.4–0.7 g) and were used for the experiments. Rats were injected under ether anesthesia with 2–3 MBq of 0.34 nmol (0.5 μg total peptide mass) ^{111}In-**3** or ^{111}In-**5** in 0.1 ml saline; the injection was given in the femoral vein.

In both animal models, rats were sacrificed under ether anesthesia 4 hr, 24 hr, and 48 hr after injection. Organs and blood were collected, and the radioactivity in these samples was determined by using a γ-counter. In order to determine the nonspecific uptake of the radiopeptides, rats were injected with 0.5 mg octreotide in 0.1 ml saline as a coinjection with the radioligand.

Statistical Methods

To compare differences between the radiopeptides, the Student's t test was used.

Supplemental Data

Supplemental Data include a table with the analytical data for compounds **1–24** and are available at http://www.chembiol.com/cgi/content/full/13/10/1081/DC1/.

Acknowledgments

M.G., J.C., and H.R.M. acknowledge support from the Swiss National Science Foundation (grant no. 3100A0-100390) and Bundesamt für Bildung und Wissenschaft (BBW, grant no. C00.0091). The analytical support provided by Novartis Pharma (Dieter Staab) as well as the expert technical assistance of K. Hinni (Basel) and D. Mayer (Magdeburg) are also gratefully acknowledged.

Received: March 23, 2006
Revised: August 4, 2006
Accepted: August 28, 2006
Published: October 20, 2006

References

1. Veber, D.F., Freidinger, R.M., Perlow, D.S., Paleveda, W.J., Jr., Holly, F.W., Strachan, R.G., Nutt, R.F., Arison, B.H., Homnick, C., Randall, W.C., et al. (1981). A potent cyclic hexapeptide analogue of somatostatin. Nature *292*, 55–58.
2. Bauer, W., Briner, U., Doepfner, W., Haller, R., Huguenin, R., Marbach, P., Petcher, T.J., and Pless, J. (1982). SMS-201–995:

a very potent and selective octapeptide analogue of somatostatin with prolonged action. Life Sci. *31*, 1133–1140.

3. Hoyer, D., Bell, G.I., Berelewitz, M., Epelbaum, J., Feniuk, W., Humphrey, P.P.A., O'Caroll, A.-M., Patel, Y.C., Schonbrunn, A., Taylor, J.E., et al. (1995). Classification and nomenclature of somatostatin receptors. Trends Pharmacol. Sci. *16*, 86–88.
4. Reubi, J.C., Laissue, J., Krenning, E., and Lamberts, S.W. (1992). Somatostatin receptors in human cancer: incidence, characteristics, functional correlates and clinical implications. J. Steroid Biochem. Mol. Biol. *43*, 27–35.
5. Reubi, J.C., Waser, B., Schaer, J.C., and Laissue, J.A. (2001). Somatostatin receptor sst1-sst5 expression in normal and neoplastic human tissues using receptor autoradiography with subtype-selective ligands. Eur. J. Nucl. Med. *28*, 836–846.
6. Reubi, J.C. (2003). Peptide receptors as molecular targets for cancer diagnosis and therapy. Endocr. Rev. *24*, 389–427.
7. Hofland, L.J., Liu, Q., Van Koetsveld, P.M., Zuijderwijk, J., Van Der Ham, F., De Krijger, R.R., Schonbrunn, A., and Lamberts, S.W. (1999). Immunohistochemical detection of somatostatin receptor subtypes sst1 and sst2A in human somatostatin receptor positive tumors. J. Clin. Endocrinol. Metab. *84*, 775–780.
8. Kulaksiz, H., Eissele, R., Rossler, D., Schulz, S., Hollt, V., Cetin, Y., and Arnold, R. (2002). Identification of somatostatin receptor subtypes *1*, 2A, *3*, and 5 in neuroendocrine tumours with subtype specific antibodies. Gut *50*, 52–60.
9. Forssell-Aronsson, E., Nilsson, O., Benjegard, S.A., Kolby, L., Bernhardt, P., Molne, J., Hashemi, S.H., Wangberg, B., Tisell, L.E., and Ahlman, H. (2000). ^{111}In-DTPA-D-Phe^{1}-octreotide binding and somatostatin receptor subtypes in thyroid tumors. J. Nucl. Med. *41*, 636–642.
10. Halmos, G., Sun, B., Schally, A.V., Hebert, F., and Nagy, A. (2000). Human ovarian cancers express somatostatin receptors. J. Clin. Endocrinol. Metab. *85*, 3509–3512.
11. Ferone, D., Van Hagen, M.P., Kwekkeboom, D.J., Van Koetsveld, P.M., Mooy, D.M., Lichtenauer-Kaligis, E., Schönbrunn, A., Colao, A., Lamberts, S.W.J., and Hofland, L.J. (2000). Somatostatin receptor subtypes in human thymoma and inhibition of cell proliferation by octreotide in vitro. J. Clin. Endocrinol. Metab. *85*, 1719–1726.
12. Mundschenk, J., Unger, N., Schulz, S., Höllt, V., Schulz, S., Stenke, R., and Lehnert, H. (2003). Somatostatin receptor subtypes in human pheochromocytoma: subcellular expression pattern and functional relevance for octreotide scintigraphy. J. Clin. Endocrinol. Metab. *88*, 5150–5157.
13. Papotti, M., Croce, S., Bello, M., Bongiovanni, M., Allia, E., Schindler, M., and Bussolati, G. (2001). Expression of somatostatin receptor types *2*, 3 and 5 in biopsies and surgical specimens of human lung tumours. Virchows Arch. *439*, 787–797.
14. Reubi, J., Schaer, J., Waser, B., Wenger, S., Heppeler, A., Schmitt, J.S., and Maecke, H.R. (2000). Affinity profiles for human somatostatin receptor sst1-sst5 of somatostatin radiotracers selected for scintigraphic and radiotherapeutic use. Eur. J. Nucl. Med. *27*, 273–282.
15. Bodei, L., Cremonesi, M., Grana, C., Rocca, P., Bartolomei, M., Chinol, M., and Paganelli, G. (2004). Receptor radionuclide therapy with 90Y-[DOTA]0-Tyr3-octreotide (90Y-DOTATOC) in neuroendocrine tumours. Eur. J. Nucl. Med. Mol. Imaging *31*, 038–046.
16. Murphy, W., Lance, V.A., Moreau, S., Moreau, J.P., and Coy, D.H. (1987). Inhibition of rat prostate tumor growth by an octapeptide analog of somatostatin. Life Sci. *40*, 2515–2522.
17. Cai, R., Szoke, B., Lu, R., Fu, D., Redding, T.W., and Schally, A.V. (1986). Synthesis and biological activity of highly potent octapeptide analogs of somatostatin. Proc. Natl. Acad. Sci. USA *83*, 1896–1900.
18. Melacini, G., Zhu, Q., and Goodman, M. (1997). Multiconformational NMR analysis of Sandostatin (octreotide): equilibrium between β-sheet and partially helical structures. Biochemistry *36*, 1233–1241.
19. Pohl, E., Heine, A., Sheldrick, G.M., Dauter, Z., Wilson, K.S., Kallen, J., Huber, W., and Pfaffli, P.J. (1995). Structure of octreotide, a somatostatin analogue. Acta Crystallogr. D Biol. Crystallogr. *51*, 48–59.
20. Deshmukh, M.V., Voll, G., Kuhlewein, A., Mäcke, H., Schmitt, J., Kessler, H., and Gemmecker, G. (2005). NMR studies reveal structural differences between the gallium and yttrium complexes of DOTA-D-Phe^{1}-Tyr^{3}-octreotide. J. Med. Chem. *48*, 1506–1514.
21. Mattern, R., Moore, S.B., Tran, T.A., Rueter, J.K., and Goodman, M. (2000). Synthesis, biological activities and conformational studies of somatostatin analogs. Tetrahedron *56*, 9819–9831.
22. Wild, D., Schmitt, J.S., Ginj, M., Mäcke, H.R., Bernard, B.F., Krenning, E.P., De Jong, M., Wenger, S., and Reubi, J.C. (2003). DOTA-NOC, a high affinity ligand of somatostatin receptor subtypes *2*, 3 and 5 for labelling with various radiometals. Eur. J. Nucl. Med. Mol. Imaging *30*, 1338–1347.
23. Lewis, I., Bauer, W., Albert, R., Chandramouli, N., Pless, J., Weckbecker, G., and Bruns, C. (2003). A novel somatostatin mimic with broad somatotropin release inhibitory factor receptor binding and superior therapeutic potential. J. Med. Chem. *46*, 2334–2344.
24. Hofland, L., Breeman, W.A., Krenning, E.P., de Jong, M., Waaijers, M., van Koetsveld, P.M., Maecke, H.R., and Lamberts, S.W. (1999). Internalization of [DOTA^{0},^{125}I-Tyr^{3}]Octreotide by somatostatin receptor-positive cells in vitro and in vivo: implications for somatostatin receptor-targeted radio-guided surgery. Proc. Assoc. Am. Physicians *111*, 63–69.
25. Hocart, S.J., Jain, R., Murphy, W.A., Taylor, J.E., Morgan, B., and Coy, D.H. (1998). Potent antagonists of somatostatin: synthesis and biology. J. Med. Chem. *41*, 1146–1154.
26. Vale, W., Rivier, C., Brown, M., and Rivier, J. (1977). Hypothalamic peptide hormones and pituitary regulation. In Advances in Experimental Medicine and Biology, J.C. Porter, ed. (New York: Plenum Press), pp. 123–156.
27. Meyerhof, W. (1998). The elucidation of somatostatin receptor functions: a current view. Rev. Physiol. Biochem. Pharmacol. *133*, 55–108.
28. Roth, A., Kreienkamp, H.J., Nehring, R.B., Roosterman, D., Meyerhof, W., and Richter, D. (1997). Endocytosis of the rat somatostatin receptors: subtype discrimination, ligand specificity, and delineation of carboxy-terminal positive and negative sequence motifs. DNA Cell Biol. *16*, 111–119.
29. Valkema, R., Froberg, A.C., Bakker, W.H., Maecke, H.M., Breeman, W.A., Kooij, P.P., de Jong, M., de Jong, L.C., and Krenning, E.P. (2005). Peptide receptor radionuclide therapy (PRRT) with Lu-177-DOTANOC and peptide receptor scintigraphy (PRS) with In-111-DOTANOC and Ga-68-DOTANOC. J. Nucl. Med. *46* (*Suppl. 2*), 151P.
30. Tulipano, G., Stumm, R., Pfeiffer, M., Kreienkamp, H.J., Hollt, V., and Schulz, S. (2004). Differential beta-arrestin trafficking and endosomal sorting of somatostatin receptor subtypes. J. Biol. Chem. *279*, 21374–21382.
31. Storch, D., Behe, M., Walter, M.A., Chen, J., Powell, P., Mikolajczak, R., and Maecke, H.R. (2005). Evaluation of [^{99m}Tc/EDDA/HYNIC^{0}]octreotide derivatives compared with [^{111}In-DOTA^{0}, Tyr^{3}, Thr^{8}]octreotide and [^{111}In-DTPA^{0}]octreotide: does tumor or pancreas uptake correlate with the rate of internalization? J. Nucl. Med. *46*, 1561–1569.
32. Stolz, B., Weckbecker, G., Smith-Jones, P.M., Albert, R., Raulf, F., and Bruns, C. (1998). The somatostatin receptor-targeted radiotherapeutic [^{90}Y-DOTA-DPhe^{1},Tyr^{3}]octreotide (^{90}Y-SMT 487) eradicates experimental rat pancreatic CA 20948 tumours. Eur. J. Nucl. Med. *25*, 668–674.
33. Pfeiffer, M., Koch, T., Schroder, H., Klutzny, M., Kirscht, S., Kreienkamp, H.J., Hollt, V., and Schulz, S. (2001). Homo- and heterodimerization of somatostatin receptor subtypes. Inactivation of sst(3) receptor function by heterodimerization with sst(2A). J. Biol. Chem. *276*, 14027–14036.
34. Pfeiffer, M., Koch, T., Schroder, H., Laugsch, M., Hollt, V., and Schulz, S. (2002). Heterodimerization of somatostatin and opioid receptors cross-modulates phosphorylation, internalization, and desensitization. J. Biol. Chem. *277*, 19762–19772.
35. Elberg, G., Hipjin, R.W., and Schonbrunn, A. (2002). Homologous and heterologous regulation of somatostatin receptor 2. Mol. Endocrinol. *16*, 2502–2514.
36. Boerman, O.C., Oyen, W.J.G., and Corstens, F.H.M. (2001). Between the Scylla and Charybdis of peptide radionuclide

therapy: hitting the tumor and saving the kidney. Eur. J. Nucl. Med. Mol. Imaging *28*, 1447–1449.

37. Ginj, M., Chen, J., Walter, M.A., Eltschinger, V., Reubi, J.C., and Maecke, H.R. (2005). Preclinical evaluation of new and highly potent analogs of octreotide for predictive imaging and targeted radiotherapy. Clin. Cancer Res. *11*, 1136–1145.
38. Bruns, C., Lewis, I., Briner, U., Meno-Tetang, G., and Weckbecker, G. (2002). SOM230: a novel somatostatin peptidomimetic with broad somatotropin release inhibiting factor (SRIF) receptor binding and a unique antisecretory profile. Eur. J. Endocrinol. *146*, 707–716.
39. IUPAC-IUB Commission of Biochemical Nomenclature (CBN) (1972). Symbols for amino-acid derivatives and peptides, recommendations 1971. Eur. J. Biochem. *27*, 201–207.
40. Heppeler, A., Froidevaux, S., Maecke, H.R., Jermann, E., Behe, M., Powell, P., and Hennig, M. (1999). Radiometal-labelled macrocyclic chelator-derivatised somatostatin analogue with superb tumour targeting properties and potential for receptor-mediated internal radiotherapy. Chem. Eur. J. *5*, 1974–1981.
41. Atherton, E., and Sheppard, R. (1989). Fluorenylmethoxycarbonyl-polyamide solid phase peptide synthesis - general principles and development. In Solid Phase Peptide Synthesis. A Practical Approach (Oxford: Oxford Information Press), pp. 25–38.
42. Schulz, S., Pauli, S.U., Schulz, S., Haendel, M., Dietzmann, K., Firsching, R., and Hoellt, V. (2000). Immunohistochemical determination of five somatostatin receptors in meningioma reveals frequent overexpression of somatostatin receptor subtype sst2A. Clin. Cancer Res. *6*, 1865–1874.